A NOVEL GRAPHIC PRESENTATION AND FRACTAL CHARACTERISATION OF POINCARÉ SOLUTIONS OF HARMONICALLY EXCITED PENDULUM

Salau T. A.O. and Ajide O.O.
Department of Mechanical Engineering, University of Ibadan, Nigeria.

ABSTRACT

The extensive completed research and continuous study of pendulum is due to its scientific and engineering importance. The present study simulate the Poincare solutions of damped, nonlinear and harmonically driven pendulum using FORTRAN90 coded form of the popular fourth and fifth order Runge-Kutta schemes with constant time step. Validation case studies were those reported by Gregory and Jerry (1990) for two damping qualities ($q_1, q_2 = 2, 4$), fixed drive amplitude and frequency ($g = 1.5, \omega_D = 2/3$). A novel graphic presentation of the displacement and velocity components of the Poincare solutions for 101-cases each drawn from the parameters spaces $2 \le q \le 4$ and $0.9 \le g \le 1.5$ at 100-equal steps were characterised using the fractal disk dimension analysis. Corresponding validation results compare well with reported results of Gregory and Jerry (1990). There is observed quantitative variations in the corresponding consecutive Poincare solutions prescribed by Runge-Kutta schemes with increasing number of excitation period however the quality of the overall Poincare section is hard to discern. Non-uniform variation of scatter plots per area of solutions space characterised chaotic and periodic responses as against average uniform variation for a random data set. The plots of periodic response distribute restrictedly on the solutions space diagonal while probabilities of chaotic responses on the studied parameters space is between 21.5% and 70.6%. Estimated fractal disk dimension variation is in the range $0.00 \le D_f \le 1.81$ for studied cases. The study therefore has demonstrated the utility of the novel graphic plots as a dynamic systems characterising tool.

KEYWORDS: *Graphic, Fractal disk dimension, Excited Pendulum, Poincare Solutions and Runge-Kutta Scheme.*

I. INTRODUCTION

Fractals are typically self-similar patterns. It generally implies a mathematical set that has a fractal dimension that is often more than its topological dimension . Fractal characterisation can refers to the approach of evaluating fractal dimension of geometry. Borodich in 2009 (As reported by Borodich and Evans, 2013) , the basic fundamentals of fractal characterisation follows from the analysis of basic concepts of fractal that real objects can be described as physical fractals. Graphic presentation is becoming an interesting platform for concise explanation of the dynamics of nonlinear systems. According to Webopedia (2013), graphic refers to any computer device or program that makes a computer capable of displaying and manipulating pictures. It is a term that that can also be described as images of an object. For example, laser printers and plotters are graphics devices because they permit the computer to output pictures. Presentation graphics software is a useful tool for creating bar charts, pie charts, graphics, and other types of images for fractal characterisation of nonlinear system dynamics. The charts can be based on data imported from spreadsheet applications. The techniques based on fractals show promising results in the field of graphic or image understanding and visualisation of high complexity data. The aim of Mihai and Klaus in 1994 was to introduce new researchers in this field to the theory of fractals. Equally, their paper presents several experiments using fractals as platform for generating accurate models for landforms and cover types, generation of synthetic images for model based picture processing, and image processing techniques for the analysis of remotely sensed images. The methods have been applied both for optical and Synthetic Aperture

Radar (SAR) image analysis. The influence of chaotic saddles in generating chaotic dynamics in nonlinear driven oscillators has been studied by Elżbieta (2005).Typical examples of the resulting multiple aspects of chaotic system behaviours, such as chaotic transient motions, fractal basin boundaries and unpredictability of the final state, are shown and discussed with the use of geometrical interpretation of the results completed by colour computer graphics. This study has demonstrated extensively the use of graphics for nonlinear dynamics presentation. Jun (2006) investigated the Chaotic dynamic of a harmonically excited Soliton System. The influence of a soliton system under an external harmonic excitation was examined. Different routes to chaos such as period doubling, quasi-periodic routes, and the shapes of strange attractors are observed by graphic illustrations. Bifurcation diagrams, the largest Lyapunov exponents, phase projections and Poincaré maps are the graphical tools employed for the presentation of this dynamic. System identification of nonlinear time-varying (TV) systems has been a discouraging task, as the number of parameters required for accurate identification is often larger than the number of data points available, and scales with the number of data points (Zhong *et al*, 2007) . The authors adopted 3-D graphical representation of TV second-order nonlinear dynamics without resorting to taking slices along one of the four axes has been a significant challenge to date. The newly developed method using the graphical representation has the potential to be a very useful tool for characterising nonlinear TV systems. Fingerprint indexing is an efficient visual technique that greatly improves the performance of automated fingerprint identification Systems. Jin (2008) proposed a continuous fingerprint indexing method based on location, direction estimation and correlation of fingerprint singular points. There have been many approaches introduced in the design of feature extraction. Based on orientation field, authors divided it into blocks to compute the Poincaré Index. According to the report of the authors, the blocks which may have singularities are detected in the block images. Image retrieval and indexing techniques has been considered by researchers to be important for efficient management of visual database. In the fractal domain, fractal code has been described by Liagbin *et al* (2008) as a contractive affine mapping that represents a similarity relation between the range block and the domain block in an image. The authors developed a new algorithm of IFS fractal code for image retrieval on the compression domain. Finally, the preceding n-frame images which are the smallest distance sum of fractal code are taken as the retrieval result. The study has further reinforces the relevant of visual (graphic or images) aids as tool for systems dynamic characterisation. Dusen *et al* (2012) performed a 'box-counting' scaling analysis on Circle Limit III and an equivalent mono-fractal pattern based on a Koch Snowflake. Previous analysis highlighted the expected graphical differences between Escher's hyperbolic patterns and the simple mono-fractal. In addition, their analysis also identifies unexpected similarities between Escher's work and the bi-fractal poured paintings of Jackson Pollock. Positive Lyapunov exponents' criteria has been used by Salau and Ajide (2013) to develop a graphic illustration (Chaos diagram) on the parameters space of 4-dimensional harmonically excited vibration absorber control Duffing's Oscillator. The chaos diagram obtained suggested preferentially higher mass ratio for effective chaos control of Duffing's Oscillator main mass. The author's paper has shown the importance of graphical presentation in the vivid explanation of the practical applications of chaos dynamics.

It is well understood from extensive literature study that induction motors are modelled by nonlinear higher-order dynamic systems of considerable complexity. According to Joachim (1995), the dynamic analysis based on the complex notation exhibits a formal correspondence to the description using matrices of axes-oriented components and yet, significant differences exist. It was further stated in the author's work that the use of complex state variables further allows the visualization of AC machine dynamics by complex signal flow graphs. The author has successfully represented the dynamics of AC machine dynamics using complex signal flow graphs. The simple structures developed have been of enormous assistance for understanding the internal dynamic processes of a machine and their interactions with external controls. Madjid et al (2013) paper studied the estimation of stability region of autonomous nonlinear forced low order system using graphical approach. The findings obtained in their study have again demonstrate the relevance of graphical presentation in the explanation of the dynamics of nonlinear systems. The understanding of the stability boundaries of transiently non-autonomous chaotic system dynamics was enriched with graphical approach as presented in the authors' work.

Significant research efforts have been made in the adoption of poincaré section for fractal characterisation of nonlinear dynamics. In a system dynamics, first recurrence map or Poincaré map, named after Henri Poincaré, is the intersection of a periodic orbit in the state space of a continuous dynamical system with a certain lower dimensional subspace, called the Poincaré section (Wikipedia,2013). More precisely, one considers a periodic orbit with initial conditions within a section of the space. One then creates a map to send the first point to the second, hence the name first recurrence map. The transversality of the Poincaré section means that periodic orbits starting on the subspace flow through it and not parallel to it. A Poincaré map can be interpreted as a discrete dynamical system with a state space that is one dimension smaller than the original continuous dynamical system. Hall *et al* (2009) studied the use of fractal dimensions in the characterisation of chaotic systems in structural dynamics. Complex partial differential equation (PDE) model, simplified PDE model, and a Galerkin approximation method were adopted. The responses of each model are examined through zero velocity Poincaré sections. To characterise and compare the chaotic trajectories, the box counting fractal dimension of the Poincaré sections is computed. The authors work has demonstrated the relevance of Poincaré sections in the fractal characterisation of structural dynamics.

Salau and Ajide (2012) paper serves as one of the major platform for the present study. The author exploited the computation accuracy of governing equations of linearly or periodically behaves dynamic system with fourth and fifth order Runge-Kutta algorithms in developing chaos diagrams of harmonically excited Duffing oscillator. Their study demonstrated the major utility of numerical techniques in dealing with real-world problems that are dominantly nonlinear. The findings of the study shows that apart from being sensitive to initial conditions, chaos is equally sensitivity to appropriate simulation time steps. The authors concluded that chaos diagram as a generating numerical tool is uniquely characterised by being faster and useful for reliable prediction of Duffing's oscillator dynamic responses.

Extensive literature review shows that significant works have not been done in the graphical presentation of the fractal dynamics of harmonically excited pendulum using poincaré solutions. This lacuna motivated the present paper with borders on the fractal characterisation of harmonically excited pendulum using poincaré sectioning approach.

This paper is divided into five main sections for the purpose of clarity of presentation. Section 1 is the background introduction to the study. Methodology, Results and Discussion, Conclusions and Future Applications of the study are presented in sections 2, 3, 4 and 5 respectively.

II. METHODOLOGY

Due to its engineering importance and its ability to exhibit rich nonlinear dynamics phenomena, harmonically excited pendulum has received extensive and continuous research interests as partly evident in Gregory and Jerry (1990). In the non-dimensional and one dimensional form the governing equation of the damped, sinusoidally driven pendulum is given by equation (1). In this equation q is the damping quality parameter, g is the forcing amplitude, which is not to be confused with the gravitational acceleration, and ω_D is the drive frequency.

$$\frac{d^2\theta}{dt} + \frac{1}{q}\frac{d\theta}{dt} + \sin(\theta) = g\cos(\omega_D t) \tag{1}$$

Simulation of equation (1) with Runge-Kutta demands its transformation under the assumptions ($\theta_1 = angular\ displacement$ and $\theta_2 = angular\ velocity$) to a pair of first order differential equations (2) and (3).

$$\dot{\theta}_1 = \theta_2 \tag{2}$$

$$\dot{\theta}_2 = g\cos(\omega_D t) - \frac{1}{q}\theta_2 - \sin(\theta_1) \tag{3}$$

The present study utilised the popular constant operation time step fourth and fifth order Runge-Kutta schemes to simulate equation (1) in the first order rate equations (2) and (3). The respective details of each scheme are provided in equations (4) to (8) and (9) to (15) substituting $y \leftarrow \theta_1, \theta_2, x \leftarrow t$ and constant time step h.

Fourth-Order Runge-Kutta Scheme

$$y_{i+1} = y_i + \frac{h}{6}\{K_1 + 2(K_2 + K_3) + K_4\} \quad (4)$$

$$K_1 = f(x_i, y_i) \quad (5)$$

$$K_2 = f(x_i + \frac{h}{2}, y_i + \frac{K_1 h}{2}) \quad (6)$$

$$K_3 = f(x_i + \frac{h}{2}, y_i + \frac{K_2 h}{2}) \quad (7)$$

$$K_4 = f(x_i + h, y_i + K_3 h) \quad (8)$$

Fifth-Order Runge-Kutta Method

$$y_{i+1} = y_i + \frac{h}{90}\{7K_1 + 32K_3 + 12K_4 + 32K_5 + 7K_6\} \quad (9)$$

$$K_1 = f(x_i, y_i) \quad (10)$$

$$K_2 = f(x_i + \frac{h}{2}, y_i + \frac{K_1 h}{2}) \quad (11)$$

$$K_3 = f(x_i + \frac{h}{4}, y_i + \frac{(3K_1 + K_2)h}{16}) \quad (12)$$

$$K_4 = f(x_i + \frac{h}{2}, y_i + \frac{K_3 h}{2}) \quad (13)$$

$$K_5 = f(x_i + \frac{3h}{4}, y_i + \frac{(-3K_2 + 6K_3 + 9K_4)h}{16}) \quad (14)$$

$$K_6 = f(x_i + h, y_i + \frac{(K_1 + 4K_2 + 6K_3 - 12K_4 + 8K_5)h}{7}) \quad (15$$

Solutions Schemes

The under-listed four distinct solution schemes were implemented in the present study.

- RK41-Constant **single** simulation time step fourth order Runge-Kutta scheme.
- RK42-Constant **double** simulation time step fourth order Runge-Kutta scheme.
- RK51-Constant **single** simulation time step fifth order Runge-Kutta scheme.
- RK52-Constant **double** simulation time step fifth order Runge-Kutta scheme.

Study Parameters

In tune with literature research interest this study focuses on the parameter plane defined by $2.0 \le q \le 4.0$ and $0.9 \le g \le 1.5$, fixed drive frequency $\omega_D = \frac{2}{3}$, and fixed simulation time step $h = \frac{T_D}{500}$ for $T_D = \frac{2\pi}{\omega_D}$. The initial conditions for all studied cases is (0, 0) and the simulation was executed for 2010-excitation periods including 10-periods of transient and 2000-periods of steady solutions.

The associated **novel** attractor of Poincare solutions were investigated for their space filling ability using fractal disk dimension characterisation, see Salau and Ajide (2012). Ten (10) systematic observation scales of disk size variation and quantity of disks required for complete covering of the attractor were made in five (5) different trials per observation scale using random number generation seed value of 9876. This process enables the determination of 'optimum' number of disks required at specified observation scale.

III. RESULTS AND DISCUSSION

Tables 1 and 2 and figures 1 and 2 give validation results for the FORTRAN programmes developed for this study. Tables 1 and 2 refer. The corresponding displacement and velocity components lack repetition with increasing number of completed excitation periods and across Runge-Kutta schemes implemented. A comparison of the corresponding periodic displacement and velocity revealed corresponding absolute deviation range of 0.0-6.2 and 0.0-3.5 respectively. However, the same corresponding qualitative Poincare patterns were formed across the numerical schemes, see figures 1 and 2. It is to be noted that the Poincare patterns in figures 1 and 2 compare excellently well with those reported by Gregory and Jerry (1990) for respective damp quality of 2 and 4, fixed excitation amplitude of 1.5 and fixed drive frequency of $\frac{2}{3}$.

Table 1: Sample steady simulated Poincare Solutions at fixed excitation amplitude and drive frequency.

No of excitation periods completed	q=2				q=4			
	RK41		RK51		RK41		RK51	
	θ_1	θ_2	θ_1	θ_2	θ_1	θ_2	θ_1	θ_2
1	-2.241	1.591	-2.241	1.591	2.194	-0.062	2.183	-0.070
2	-0.588	2.277	-0.588	2.277	1.715	2.365	2.909	0.788
3	1.076	1.944	1.076	1.944	1.324	2.221	2.910	0.578
4	-2.450	1.438	-2.450	1.438	-0.449	2.804	-0.825	0.772
5	2.521	0.431	2.521	0.431	-1.280	2.058	-0.283	2.838
6	-2.750	1.217	-2.750	1.217	-0.600	0.760	-0.487	1.690
7	0.343	0.278	0.343	0.278	-2.898	0.982	0.698	-0.278
8	-0.011	1.426	-0.011	1.426	1.722	1.850	1.870	-0.238
9	-2.616	1.283	-2.616	1.283	-0.976	2.130	-0.081	-0.363
10	0.607	0.067	0.606	0.068	-0.658	0.861	1.909	-0.240
11	0.001	1.380	0.001	1.380	-1.637	2.229	-0.076	-0.374
12	2.103	0.190	2.104	0.191	-0.617	0.709	1.934	-0.224
13	0.787	2.226	0.893	2.171	0.655	-0.476	-0.026	-0.414
14	-2.644	1.298	-2.961	1.054	2.717	0.358	2.040	-0.156
15	0.619	0.061	0.149	0.559	-1.200	1.565	1.268	-0.585
16	0.001	1.378	-0.028	1.443	1.826	-0.032	3.025	0.621
17	2.064	0.170	-2.086	1.664	0.610	-0.650	-0.170	-0.071
18	0.074	1.400	-0.034	2.176	-2.912	0.897	1.479	-0.470
19	-2.909	1.060	1.012	2.020	1.872	1.776	1.696	-0.319
20	0.157	0.541	-2.382	1.494	-0.475	1.612	0.279	-0.501

Table 2: Sample steady simulated Poincare Solutions at fixed excitation amplitude and drive frequency continued

No of excitation periods completed	q=2				q=4			
	RK42		RK52		RK42		RK52	
	θ_1	θ_2	θ_1	θ_2	θ_1	θ_2	θ_1	θ_2
1	-2.241	1.591	-2.241	1.591	2.184	-0.069	2.183	-0.070
2	-0.588	2.277	-0.588	2.277	-2.381	1.643	-3.103	1.019
3	1.076	1.944	1.076	1.944	1.192	-0.295	1.756	1.786
4	-2.450	1.438	-2.450	1.438	1.398	-0.470	-1.282	2.049
5	2.521	0.431	2.521	0.431	1.913	-0.215	-0.606	0.714
6	-2.750	1.217	-2.750	1.217	-0.015	-0.421	2.398	0.182
7	0.343	0.278	0.343	0.278	2.062	-0.141	-0.239	0.367
8	-0.011	1.426	-0.011	1.426	2.137	-0.163	2.187	-0.115

9	-2.616	1.283	-2.616	1.283	-2.593	0.999	1.110	-0.461
10	0.606	0.068	0.606	0.068	1.519	2.136	2.524	0.215
11	0.001	1.380	0.001	1.380	1.554	2.525	-0.747	1.236
12	2.104	0.191	2.104	0.191	1.337	2.242	1.218	2.470
13	0.886	2.175	0.892	2.172	0.034	2.891	1.873	1.693
14	-2.942	1.068	-2.957	1.056	1.344	2.633	-2.271	1.497
15	0.156	0.544	0.150	0.556	1.418	2.140	-3.061	1.005
16	-0.027	1.444	-0.028	1.443	-0.231	0.742	1.832	1.773
17	-2.039	1.695	-2.077	1.670	-1.162	1.275	-0.831	2.113
18	0.087	2.022	-0.001	2.149	0.397	2.772	-0.659	0.880
19	1.211	1.848	1.041	1.998	1.479	2.568	1.038	2.743
20	-2.414	1.471	-2.414	1.471	1.361	2.213	1.556	1.919

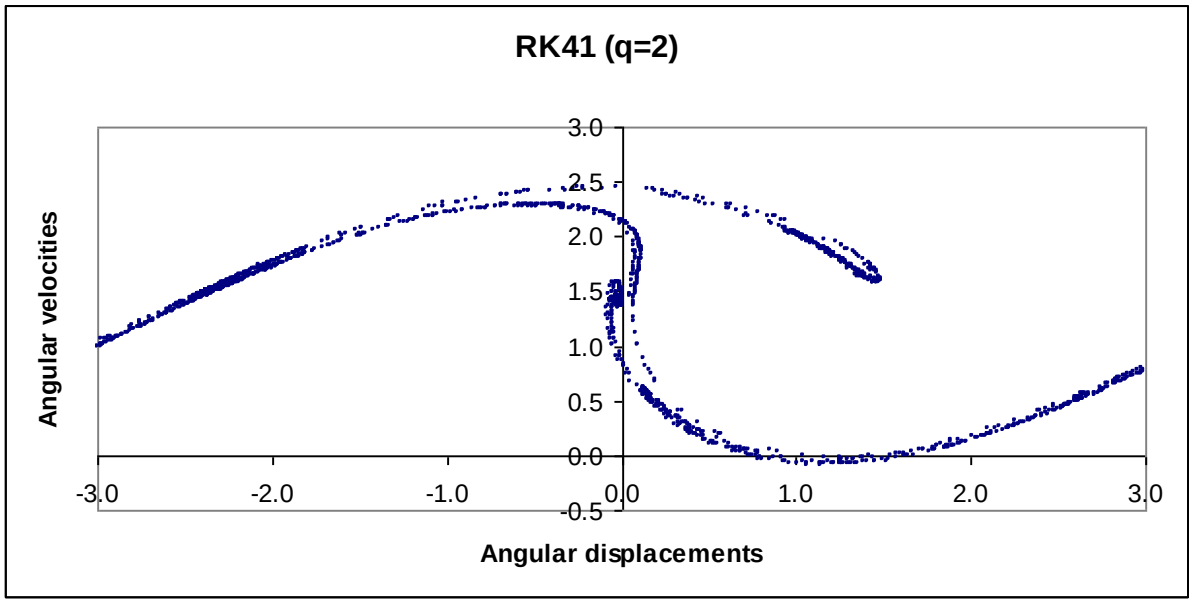

Figure 1: Poincare section of harmonically excited pendulum by RK41 and for q=2, g=1.5 and $\omega_D = \frac{2}{3}$

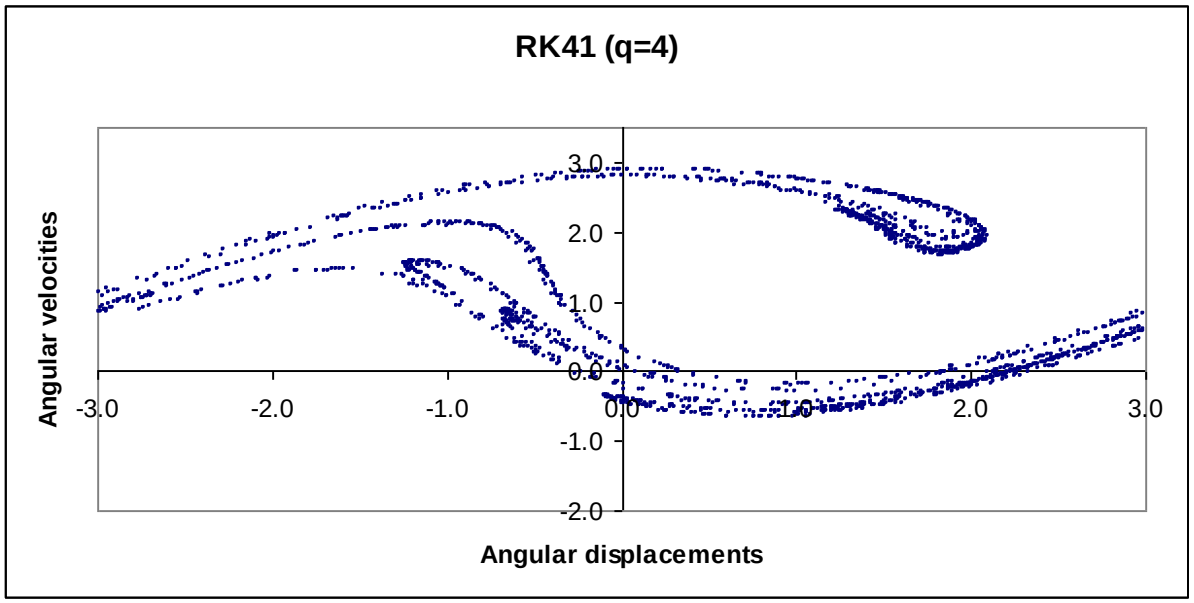

Figure 2: Poincare section of harmonically excited pendulum by RK41 and for q=4, g=1.5 and $\omega_D = \frac{2}{3}$

Figures 1 and 2 refer. Each Poincare section compare excellent well in quality with corresponding result reported by Gregory and Jerry (1990). In addition, the quality of the corresponding Poincare section is found to be the same for the Runge-Kutta schemes tagged RK42, RK51 and RK52. Furthermore, the visual assessment of the Poincare sections shows that the filling of the phase space increases with increasing damping quality and vice versa.

Does scatter plot of the displacement/velocity components of Poincare section obtained by multiple Runge-Kutta schemes produce an attractor? Answering this ponderous question is the focus of figures 3 to 6.

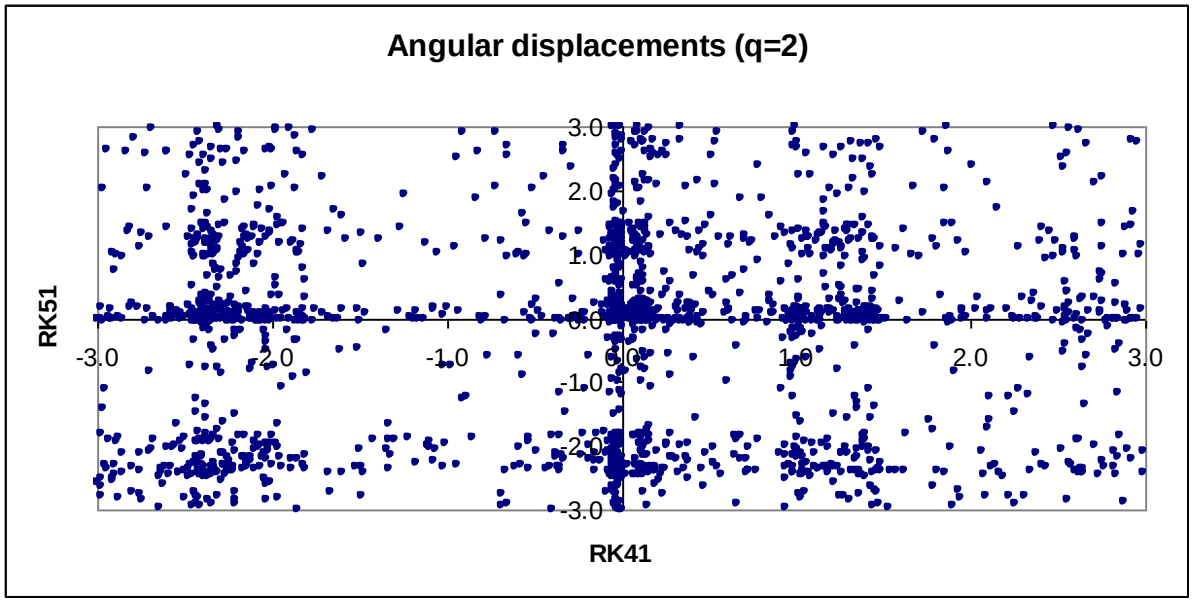

Figure 3: Scatter plot of angular displacement components (**Poincare section**) of harmonically excited pendulum by RK41 vs. RK51 and for q=2, g=1.5 and $\omega_D = \frac{2}{3}$.

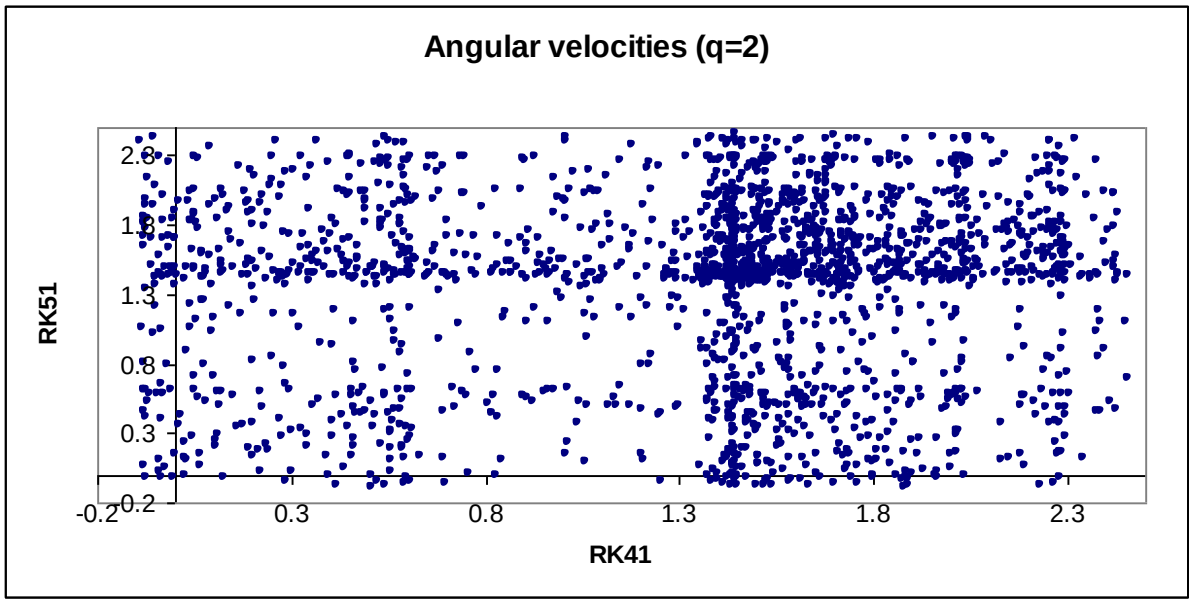

Figure 4: Scatter plot of angular velocity components (**Poincare section**) of harmonically excited pendulum by RK41 vs. RK51 and for q=2, g=1.5 and $\omega_D = \frac{2}{3}$.

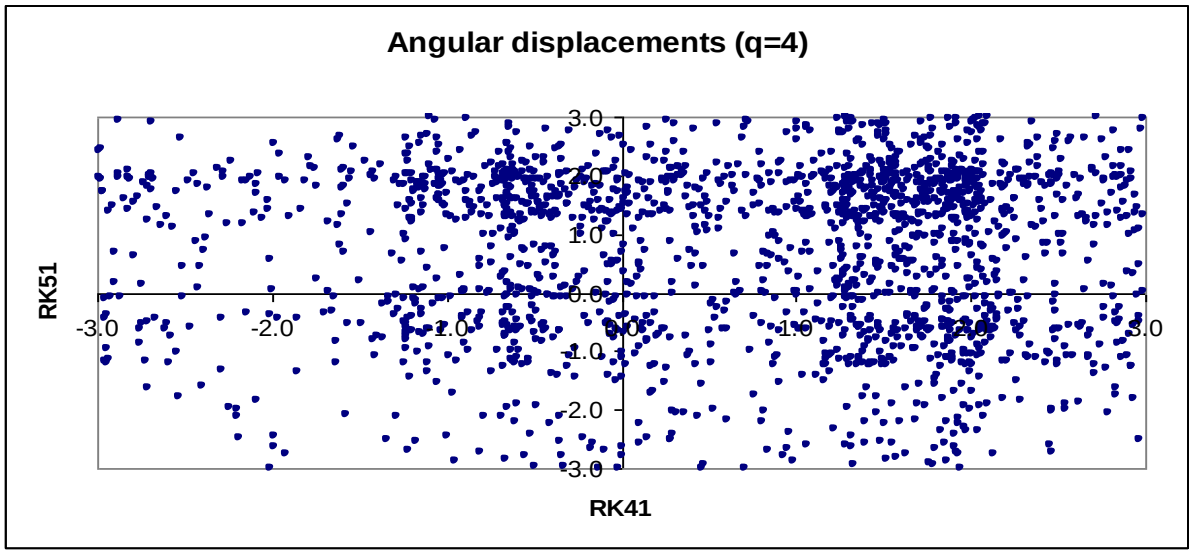

Figure 5: Scatter plot of angular displacement components (**Poincare section**) of harmonically excited pendulum by RK41 vs. RK51 and for q=4, g=1.5 and $\omega_D = \frac{2}{3}$.

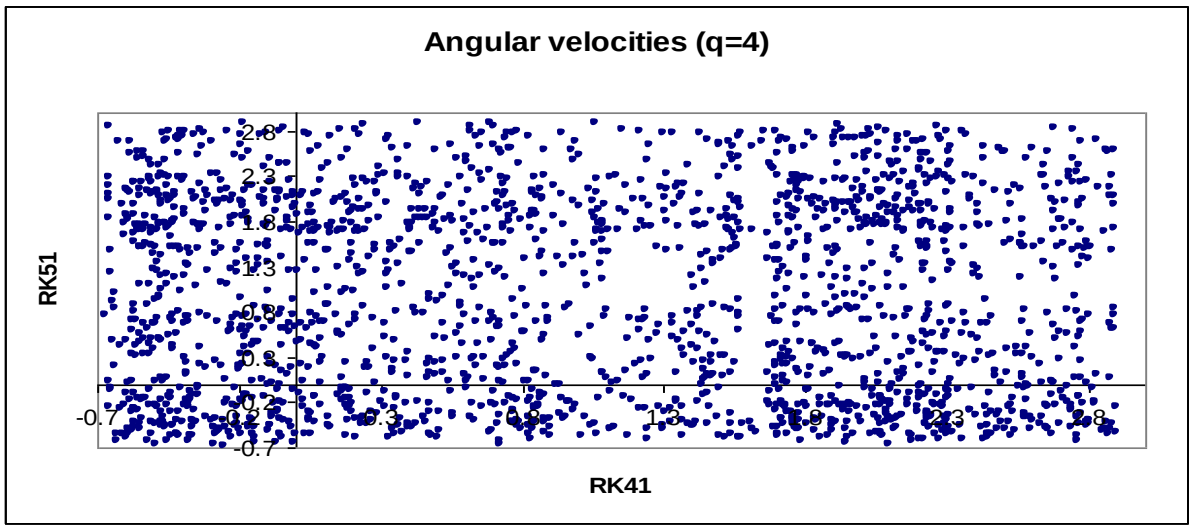

Figure 6: Scatter plot of angular velocity components (**Poincare section**) of harmonically excited pendulum by RK41 vs. RK51 and for q=4, g=1.5 and $\omega_D = \frac{2}{3}$.

Figures 3 to 6 refer. Similar corresponding scatter plots with RK41 vs. RK42 and RK51 vs. RK52 reveals qualitatively the same non-uniform distributed structural details. The scatter plots distribution per unit space area varies non-uniformly from one location to another. Is this observation a coincidence or validity in general for chaotic response of harmonically excited pendulum? It is to be noted that Gregory and Jerry (1990) reported chaotic response of the excited pendulum when driven by g=1.5, $\omega_D = \frac{2}{3}$ and for q=2 or 4. Figures 7 and 8 serve as response to this research question. Figure 7 examined the structure of known random data set on a plane while figure 8 examined harmonically excited pendulum with parameters that guarantee periodic response, see Gregory and Jerry (1990).

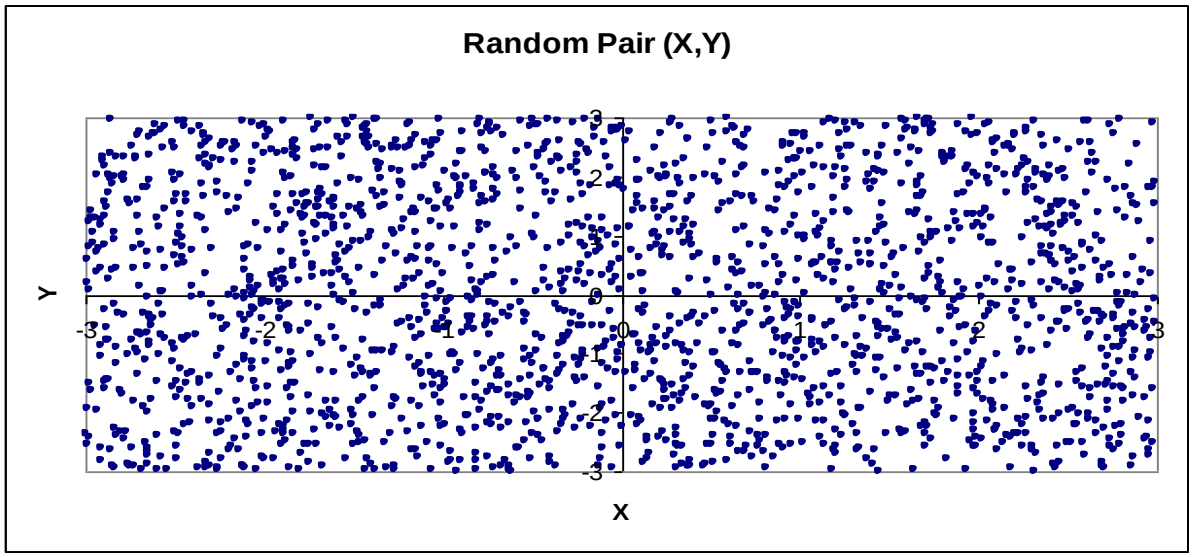

Figure 7: Scatter plot of pair of randomly generated angular displacements (X, Y): ($-3 \le (X,Y) \le 3$), $X,Y = -3 + 6 \times ran(iseed)$ and iseed=9076.

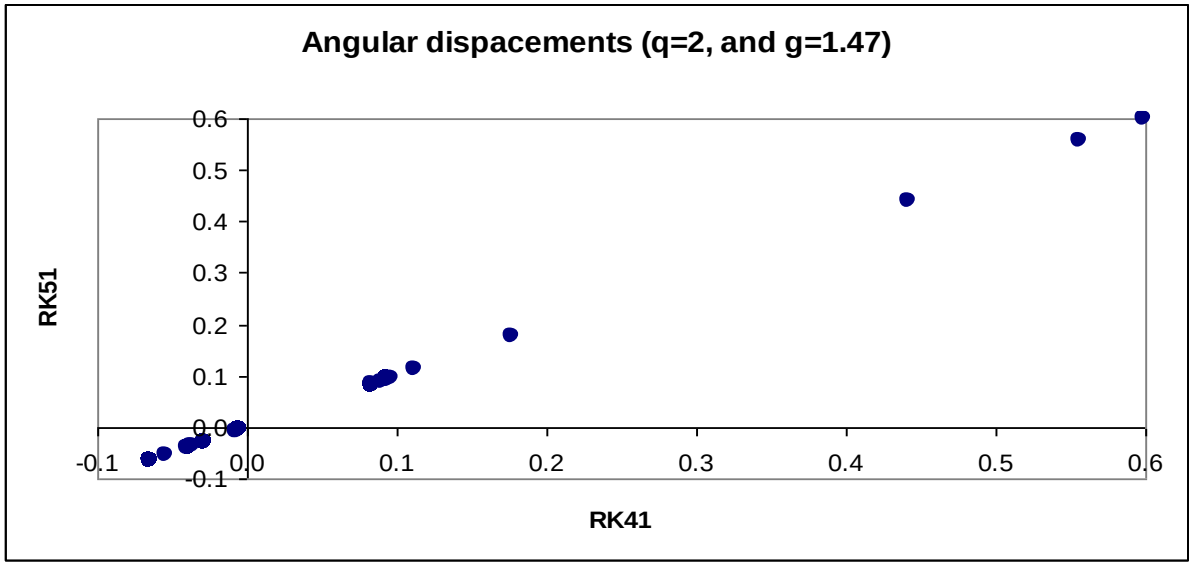

Figure 8: Scatter plot of angular displacement components (**Poincare section**) of harmonically excited pendulum by RK41 vs. RK51 and for q=2, g=1.47 and $\omega_D = \frac{2}{3}$.

It is worth to note that the scatter plot of angular velocity components (**Poincare section**) of harmonically excited pendulum by RK41 vs. RK51 and for q=2, g=1.47 and $\omega_D = \frac{2}{3}$ compare qualitatively with figure 8. Also important to note that figures 3 to 8 can be classified uniquely into three distinct groups: the data source dynamics response is chaotic (**figures 3 to 6**), the data source dynamics is random (**figure 7**) and the data source dynamics is periodic (**figure 8**). In figures 3 to 6, the distribution of the scatter plot per unit space area is non-uniform. In figure 7, the distribution of the scatter plot per unit space area is on the average uniform. In figure 8 the scatter plots distribute non-uniformly and the distribution restricted to the diagonal of the solutions space. Therefore, chaotic response manifestation is like as in any of figures 3 to 6 or its equivalent depending on pendulum driven parameters. In addition, a strong indication of periodic response is the scatter plots distribution restriction to solutions space diagonal uniformly or not.

Fractal disk dimension characterisation using disk counted method of the scatter plots such as in figures 3 to 6 and figure 8 when the damping quality or the excitation amplitude is varied and keeping other driven parameters constant is the focus of tables 3 and 4 and figures 9 to 11.

Table 3: Sample variation of estimated fractal disk dimension with increasing damping quality fixed excitation amplitude (g=1.5) and drive frequency ($\omega_D = \frac{2}{3}$).

Damping quality (q)	Estimated fractal disk dimension of the scatter plots					
	RK41 vs. RK51		RK41 vs. RK42		RK51 vs. RK52	
	θ_1	θ_2	θ_1	θ_2	θ_1	θ_2
2.00	1.76	1.77	1.76	1.68	1.60	1.63
2.04	0.28	0.34	0.28	0.34	0.28	0.34
2.08	0.91	0.87	0.53	0.80	1.37	1.22
2.12	1.61	1.72	1.70	1.72	1.67	1.59
2.16	0.13	0.21	0.13	0.21	0.13	0.21
2.20	0.13	0.00	0.13	0.00	0.13	0.00
2.24	0.13	0.00	0.13	0.00	0.13	0.00
2.28	0.13	0.00	0.13	0.00	0.13	0.00
2.32	0.13	0.12	0.13	0.12	0.13	0.12
2.36	0.13	0.24	0.13	0.24	0.13	0.24
2.40	0.13	0.23	0.13	0.23	0.13	0.23
2.44	0.13	0.20	0.13	0.20	0.13	0.20
2.48	0.17	0.20	0.17	0.20	0.17	0.20
2.52	0.42	0.20	0.42	0.20	0.42	0.20
2.56	0.24	0.20	0.24	0.20	0.24	0.20
2.60	1.66	1.65	1.56	1.64	1.55	1.62
2.64	1.72	1.66	1.73	1.67	1.73	1.63
2.68	1.71	1.64	1.55	1.76	1.59	1.64
2.72	1.76	1.64	1.64	1.63	1.68	1.65
2.76	1.63	1.66	1.62	1.63	1.62	1.65

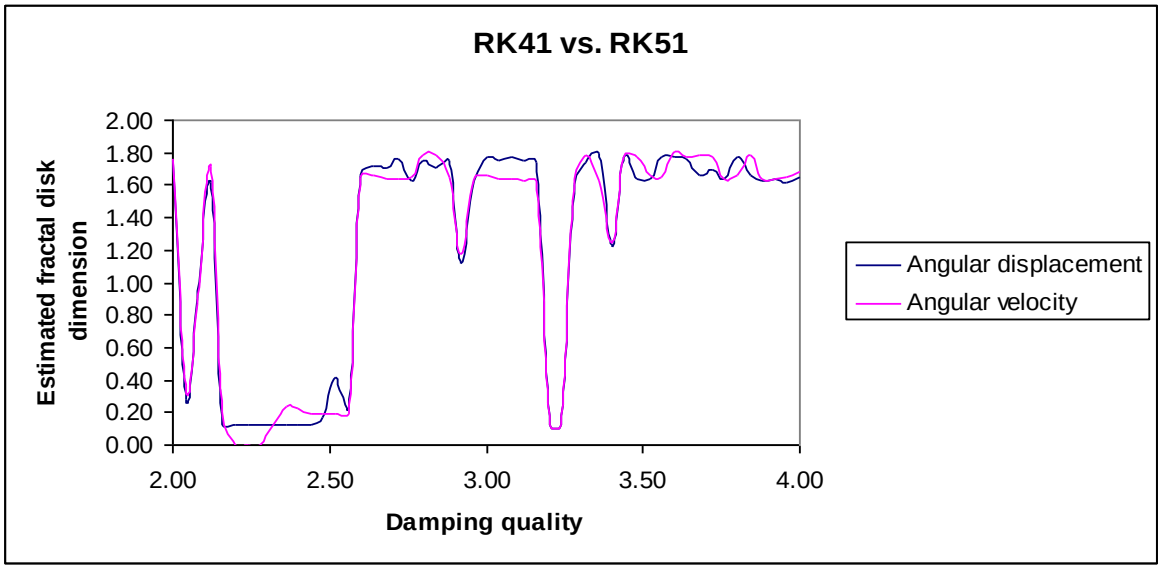

Figure 9: Variation of estimated fractal disk dimension with increasing damping quality fixed excitation amplitude (g=1.5) and drive frequency ($\omega_D = \frac{2}{3}$).

Figure 9 refers the variation of estimated fractal disk dimension trend for both angular displacement and velocity components are almost the same and vary between 0.00 and 1.80. The probability of the

estimated fractal disk dimension being greater than unity is 70.6%. Thus the chance of chaotic response when the damping quality varies between the limits of 2 and 4 is 70.6% assuming that the dimension of greater than unity implies chaotic response. Furthermore, the corresponding plot of variation of fractal disk dimension with increasing damping quality for RK41 vs. RK42 and RK51 vs. Rk52 are qualitatively the same.

Table 4: Sample variation of estimated fractal disk dimension with increasing excitation amplitude and fixed drive frequency ($\omega_D = \frac{2}{3}$).

Excitation amplitude	Estimated fractal disk dimension of the scatter plots			
	RK41 vs. RK51 (q=2)		RK41 vs. RK51 (q=4)	
	θ_1	θ_2	θ_1	θ_2
0.900	0.00	0.00	1.51	1.66
0.912	0.00	0.00	0.23	0.57
0.924	0.00	0.00	0.25	0.23
0.936	0.00	0.00	0.22	0.13
0.948	0.00	0.00	0.29	0.27
0.960	0.00	0.00	0.41	0.41
0.972	0.12	0.00	0.00	0.44
0.984	0.52	0.35	0.62	0.62
0.996	0.71	0.58	0.53	0.54
1.008	0.72	0.53	1.28	1.62
1.020	0.40	0.00	1.63	1.77
1.032	0.30	1.01	1.63	1.63
1.044	0.00	0.00	1.77	1.64
1.056	0.54	0.56	1.75	1.67
1.068	0.81	0.79	1.64	1.79
1.080	0.20	0.13	1.66	1.65
1.092	0.26	0.13	1.78	1.66
1.104	0.32	0.13	1.64	1.78
1.116	0.45	0.13	1.61	1.62
1.128	0.65	0.77	0.40	0.27

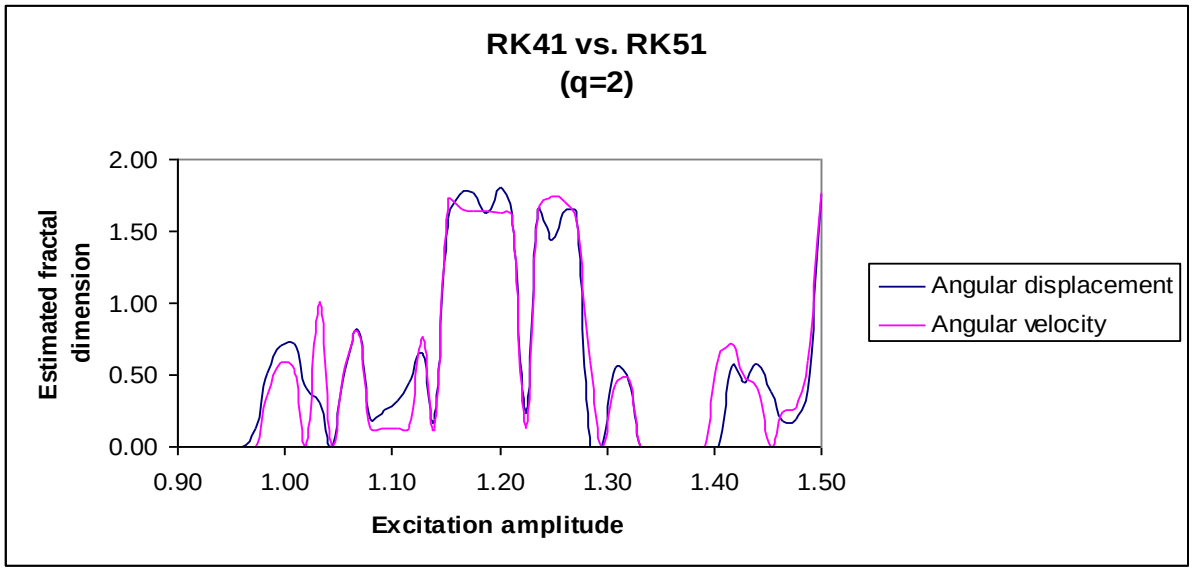

Figure 10: Variation of estimated fractal disk dimension with increasing excitation amplitude, fixed damping quality (q=2) and drive frequency ($\omega_D = \frac{2}{3}$).

Figure 10 refers the variation of estimated fractal disk dimension trend for both angular displacement and velocity components are almost the same and vary between 0.00 and 1.81. The probability of the estimated fractal disk dimension being greater than unity is 21.5%. Thus the chance of chaotic response when varying the excitation amplitude between the limits of 0.90 and 1.50 is 21.5% assuming that the dimension of greater than unity implies chaotic response. Furthermore, the corresponding plot of variation of fractal disk dimension with increasing excitation amplitude for RK41 vs. RK42 and RK51 vs. Rk52 are qualitatively the same.

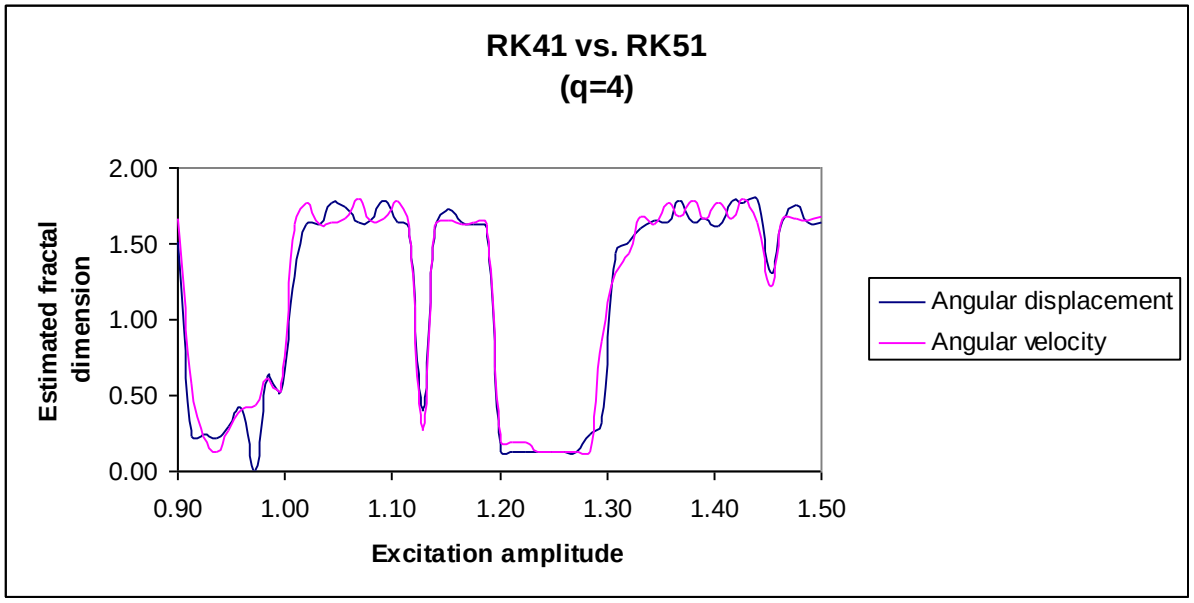

Figure 11: Variation of estimated fractal disk dimension with increasing excitation amplitude, fixed damping quality (q=4) and drive frequency ($\omega_D = \frac{2}{3}$).

Figure 11 refers. The variation of estimated fractal disk dimension trend for both angular displacement and velocity components are almost the same and vary between 0.00 and 1.79. The probability of the estimated fractal disk dimension being greater than unity is 64.7%. Thus the chance of chaotic response when varying the excitation amplitude between the limits of 0.90 and 1.50 is 64.7% assuming that the dimension of greater than unity implies chaotic response. Furthermore the corresponding plot of variation of fractal disk dimension with increasing excitation amplitude for RK41 vs. RK42 and RK51 vs. Rk52 are qualitatively the same. Though figures 11 and 9 are quantitatively different they compare significantly in qualitative term.

Referring to figures 9 to 11, it can be deduced that the probability of chaotic response of the pendulum when driven by parameters combination from plane defined by $2.0 \le q \le 4.0$ and $0.9 \le g \le 1.5$ for fixed drive frequency $\omega_D = \frac{2}{3}$ is between 21.5% and 70.6%.

IV. CONCLUSIONS

A comparison of the corresponding periodic displacement and velocity of the validation cases across Runge-Kutta schemes revealed corresponding absolute deviation range of 0.0-6.2 and 0.0-3.5 respectively. These observed quantitative variations in the corresponding consecutive Poincaré solutions prescribed by different Runge-Kutta schemes with increasing number of excitation period notwithstanding the overall quality of the Poincaré section obtained is hard to discern for all studied cases. There are three classifications of scatter plots: A non-uniform variation of scatter plots per area of solutions space characterised chaotic responses, uniform variation characterised random data set. Lastly the characterisation of periodic response is restricted distribution on the solutions space with a straight line pattern. In addition to this visual assessment of the relevant novel plots fractal

characterisation analysis revealed variation of estimated fractal disk dimension for both angular displacement and velocity components in between 0.00 and 1.81. The probabilities of chaotic responses on the studied parameters space is between 21.5% and 70.6%. The study therefore has demonstrated the utility of the novel graphic plots as a dynamic systems characterizing tool.

V. FUTURE APPLICATIONS

The future engineering applications of this study as a diagnosing tool are numerous.

- It can be used to determine whether a fluid flow is laminar or turbulence. A graphical plot of flow meter velocities data at two arbitrarily close points can be explored to distinguish a laminar flow from turbulence one.
- This graphical presentation studied can be applied in weather forecasting. A graphical plot can easily be produced from weather data (meteorological data) collected for arbitrary two close points over a period of time.
- This study will be a versatile diagnosing tool for distinguishing heat transfer characteristics in a composite and non-composite materials (whether homogeneous or not). For instance the characteristics of heat transfer (including temperature) are expected to experience irregular changes from location to location for a non-homogeneous material. Under usage such a material will tend to behaves nonlinearly

REFERENCES

[1]. Borodich F.M. and Evans H.P.(2013),Fractal characterisation of surfaces. Engineering Encyclopedia of Tribology , Springer Reference,Springer.
[2]. Dusen B.V.,Scannell B.C. and Taylor R.P.(2012),A fractal comparison of M.C. Escher's and H. von Koch's Tesselations. Fractals Reseacrh,pp.1-16,ISBN 978-0-9791874-6-9
[3]. Elżbieta T. (2005), On the role of chaotic saddles in generating chaotic dynamics in nonlinear driven oscillators. International Journal of Bifurcation and Chaos, Vol.15,Issue 4.DOI:10.1142/S0218127405012727
[4]. Gregory L. B. and Jerry P. G. (1990), Chaotic dynamics: An Introduction, Cambridge University Press, USA, pp.3-5 & 40-75.
[5]. Hall E.,Kessler S. and Hanaguds S.(2009),Use of Fractal Dimension in the Characterization of Chaotic Structural Dyanamic Systems.Applied Mechanics Reviews,Vol.44, Issue 11,S107-S113(Nov.01, 1991). Doi: 10.1115/1.3121342.Appear online: April 30, 2009.
[6]. Jin B.,Tang H.P. and Xu M.L.(2008),fingerprint singular point detection algorithms by Poincare index. Journal of World Scientific and Engineering Academy (WSEAS) Transactions on systems,vol.7,Issue 12,pp.1453-1462.Winconsin,USA.
[7]. Joachim H. (1995), The Representation of AC machine dynamics of complex signal flow graphs, IEEE transactions on industrial electronics,Vol.42, No. 3, pp. 263-271.
[8]. Jun Y.,Zhang W. and Gao X. (2006),Chaotic motion in a harmonically excited soliton system.Commun.Theor.Physics,Vol.46,pp.1-4,Beijing China, July 15,2006.
[9]. Liangbin Z.,Wang Yi,Lifeng Xi, Kun G. and Tianyun Hu. (2008),New method of image retrieval using fractal code on the compression domain. WSEAS Transactions Systems,Vol.7, Issue 12,pp.1484-1493.Winconsin,USA.
[10]. Madjid K., Hacene H. and Said G. (2013), Stability boundaries of transiently non-autonomous chaotic nonlinear system : Graphical Approach . Chaos and Complex Systems, Proceedings of the 4th international interdisciplinary chaos symposium. pp. 47-57, Springer Berlin Heidelberg. Print ISBN : 978-3-642-33914-1
[11]. Mihai D. and Klaus S.(1994),Fractal and Multiresolution Techniques for the Understanding of Geo-Information.JRC/EARSeL: Expert Meetings on Fractals,Ispra/Italy.
[12]. Salau T.A.O. and Ajide O.O. (2012), Development of chaos diagram using linearity and nonlinearity characteristics of periodic and chaotic responses. International Journal of Engineering and Technology (IJET), Vol.2, No.9,pp. 1529-1538, ISSN 2049-3444.
[13]. Salau T.A.O. and Ajide O.O.(2013),Chaos diagram of harmonically excited vibration absorber's control duffing's oscillator. International Journal of Scientific and Engineering Reseacrh,Vol.4, Issue 1,ISSN 2229-5518.

[14]. Salau, T.A.O. and Ajide, O.O. (2012), Disk and Box Dimensions: Selected Case Studies of Fractals with IFS Codes, International Journal of Sciences and Technology (IJST), Volume 1, No. 5, pp.234-247.
[15]. Webopedia (2013), Graphics. It is extracted from http://www.webopedia.com/TERM /G/graphics.htm. The article is downloaded from the website on 23rd April 2013.
[16]. Wikipedia (2013), Poincaré map. This article is extracted from http://en.wikipedia.org /wiki/poincaré_ map. It is downloaded from the Wikipedia (a free encyclopedia) website on 23 rd April 2013.
[17]. Zhong Y., Jan K., Ju K. and Chon K. (2007), Representation of time-varying nonlinear systems with time-varying principal dynamic modes. IEEE trans Biomed Eng.,Vol.54 (11): 1983-92

AUTHORS PROFILE

Salau Tajudeen Abiola Ogunniyi is a senior lecturer in the department of Mechanical Engineering, University of Ibadan, Nigeria. He was appointed by the University of Ibadan in February 1993 as Lecturer-II. By dint of hard work and his outstanding service contributions to the department, he was promoted to position of Lecturer-I in 2002 and Senior Lecturer in 2008. He had served the department in various capacities. He was the coordinator of the department for 2004/2005 and 2005/2006 academic sessions. He was the recipient of M.K.O Abiola postgraduate scholarship in 1993/94 academic session while on his Ph.D research programme at the University of Ibadan, Nigeria. Salau has many publications in scholarly journals and conference proceedings. His keen area of specialization is solid mechanics with bias in nonlinear dynamics (Chaos systems modelling and Fractal Characterisation). Salau is a corporate member, Nigerian Society of Engineers (NSE) and a registered Engineer by Council for Regulations of Engineering in Nigeria (COREN).He is happily married and blessed with children.

Ajide Olusegun Olufemi is currently a Lecturer-II in the department of Mechanical Engineering, University of Ibadan, Nigeria. He was appointed by the University as Lecturer-II on 1st December 2010.Until his appointment as Lecturer-II, he has worked as the Project Site Engineer/Manager of PRETOX Engineering Nigeria Ltd., Nigeria. Ajide obtained B.Sc (Honours) in 2003 from the Obafemi Awolowo University, Ile-Ife, Nigeria and M.Sc from the University of Ibadan, Ibadan, Nigeria. He received the prestigious Professor Bamiro Prize (Vice Chancellor Award) in 2008 for the overall best M.Sc student in Mechanical Engineering (Solid Mechanics), University of Ibadan, Nigeria. He has more than fifteen publications in international journals and scholarly conference proceedings. His research interest includes solid mechanics, Materials Engineering and Applied Mechanics. Ajide is a COREN registered Engineer. In addition, he is a corporate member of the Nigerian Society of Engineers (NSE) as well as corporate member Nigerian Institution of Mechanical Engineers (NIMechE).